CHAPTER 2

Effect of solvent gradient inside the entropic trap on polymer migration

2.1 Introduction

In the cell, movement of nucleotides, proteins, polysaccharides hold ubiquitous significance [9, 15]. The dynamical processes of translocation of DNA and RNAs occur within the shortest length and time scale. Ejection of DNA from viral capsid, mRNA transport through the nuclear membrane, translocation of nascent polypeptides through the endoplasmic reticulum, etc. are to name a few in a large array of migration or translocation processes in living organisms [50, 51]. The migration process of molecules within the cell/nucleus is far from complex and involves a cascade of processes.

W. H. Couter [52] invented a device with pair of electrodes across an orifice filled with an electrolyte solution. Usually, it shows current reading in the electrometer due to the ionic solution. Whenever a molecule migrates through the pore, it blockades the current flow. DNA or polymer sequencing through the nanopore is solely based on studying the current signal. The migration of polymer through a narrow constriction may be used for sequencing [53–55]. The primary motivation of nanopore sequencing studies comes from the goal of reading the whole human genome sequence [56]. Polymer migration studies can bring new dimensions to customized drug deliveries, gene therapy, biological sensing processes also [57, 58].

Though it seems straightforward to read the nucleotides from the

current signal, polymer translocation entails many challenges in reality [59]. Stochastic diffusion and fast migration often lead to erroneous sequencing. The general picture that emerges is for accurate reading of bases, slow migration of polymer must be ensured [57]. The polymer migration time generally depends on the length of the polymer, applied external voltage, chemical and physical property of pore, etc [57]. These are broadly classified into two categories: (i) influence of geometrical trapping, and (ii) field mediated migration. The free energy of a single polymer with N independent configurations can be written as $F = E - TS = E - T\log(N)$, where E is the interactive energy due to monomer attractions. Now, in geometrical trapping polymer experiences a restricted environment while threading inside the pore and loses a large number of configurations [60]. This eventually increases the free energy and forms a barrier across the pore [61, 62]. This is also known as the entropic barrier. Single molecule studies revealed that the migration process is delayed due to microfluidic channels (geometric confinements) which enhances the readability of the sequence [63, 64]. Lam et. al. [65] proposed the use of ultrathin nanoporous silicon nitride membranes as entropic traps to confine polymers for long times within the nanochannel. Whereas field induced polymer migrations are mostly dominated by the applied electric field or chemical gradient across the pore [66, 67]. Wang and Muthukumar [68] experimentally observed that the translocation process of RNA inside a α-hemolysin protein pore was affected by the pH-gradient across the pore. The presence of pH gradient (or solvent gradient) arises due to the protonation of charged amino acid residues inside the pore. Buyukdagl et al [69] showed that inclusion of pressure gradient in a driven polymer migration results in extended migration time. Tsutsui et al [70] experimentally observed that a transverse electric field in a silicon di-oxide nanochannel slowed down the biopolymer migration velocity.

Migrations induced by chemical gradients along the migration axis often forms globules in the poor solvent side and this globule acts as a

ratchet to attract more segments from the good side [71, 72]. The manipulation of the solvent quality in presence of patchy channel makes the translocation fast which helps in drug delivery through dendritic carrier molecules [73]. Noteworthy and complex phenomenon happens when solvent gradient or dielectric constant gradient is introduced in transverse fashion within the nanopore such that the solvent quality differs along the perpendicular direction of the migration axis. Ajdari and Prost [74] theoretically predicted that DNA confined in a geometrical trap with transverse gradient field in addition to uniform field along the flow may confine DNA within the trap. Regtmeier[75] experimentally verified the findings of Ajdari and Prost [74] by taking an inhomogeneous field along with a constant field, which results in slow migration.

The chemical gradient inside the nanopore channel either in the horizontal or transverse directions may have different effects on polymer migration and be involved in different biological implications. Motivated by this, we study the polymer migration through an entropic trap in presence of the gradient in the horizontal as well as in the transverse direction. In order to model the horizontal and the transverse gradient field, we consider a varying non-bonded nearest neighbor attraction among the monomers (ϵ). Here, we focus ourselves mostly on the issues where the effective change in non-bonded nearest neighbor interaction (gradient field) hinders the uniform migration in the framework of quasi-equilibrium statistical mechanics.

A large number of theoretical and simulation studies describing the complexity of the migration process rely on the quasi-equilibrium approach [76–78]. In theoretical quasi-static migration studies, where the time taken by each successful migration step is greater than the relaxation time of the polymer, one can use Fokker-Planck equation [79–81] to calculate the migration time. In such approach the migration is usually unidirectional. It is further assumed that the movement of polymer is slow enough so that the diffusion coefficient of polymer can be considered as a constant parameter throughout the process [81].

The aim of the present chapter is to illustrate the role of the solvent interaction gradient ($\Delta\epsilon$) in presence of an entropic trap on the migration. The chapter is organized as follows. In section 2.2, we briefly describe the model and method used to study the migration of polymer through the channel in presence of an entropic trap. In section 2.3, we obtain the free-energy landscape and calculated the associated migration time. We have calculated the x and y- component of radius of gyration to study the configurational properties of the polymer during the migration in Section 2.4. A summary of this work has been presented in section 2.5.

2.2 Model and Method

In this study, we model a polymer chain migrating through a non-uniform channel with and without an entropic trap. The solvent interaction gradient varying along x and y direction are shown in Fig. 2.1(a-b) and Fig. 2.1 (c-d). respectively. First, we model the polymer chain as self-attracting-self-avoiding walk (SASAW) on a square lattice [82–85]. Monomers are sites occupied by the polymers, and interactions are among non-bonded nearest neighbour monomers. The thermodynamic properties of a polymer chain in a solvent of uniform quality is expressed in the form of averages of the physical observables derived from the partition function. The canonical partition function for the polymer chain of length N in a homogeneous system can be written as

$$Z = \sum_{all\ walks} \tau^{N_p} \tag{2.1}$$

The summation is over all the possible walks and $\tau = \exp(-\beta\epsilon)$ is the Boltzmann weight corresponding to the non-bonded nearest neighbor. Here, $\beta = \frac{1}{K_B T}$, where K_B is the Boltzmann constant and T is the temperature. N_p is the number of nearest neighbor pairs, where each pair has energy ϵ. In this work, we have taken the chain length $N = 28$. We also set $K_B = 1$ and $-1 < \epsilon < 0$ from here onward.

In order to study the effect of free energy barriers arising due to in-

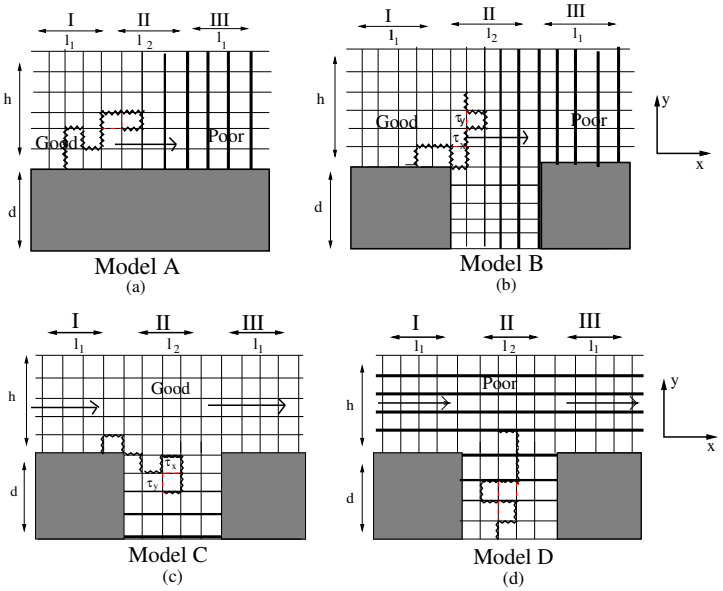

Figure 2.1. Schematic representations of polymer chain migration through an inhomogeneous channel. Channel has three different regions (I, II, and III) of a certain length ($l_1 = 14, l_2 = 10$ lattice units) width ($h = 12$ lattice units) and different solvent quality (good, poor, and solvent): (a) Model A: Channel without entropic trap and solvent interaction gradient (in region II) is along the x-direction; (b) Model B: Channel with entropic trap of depth $d = 10$ lattice units and solvent interaction gradient (in region II) is along the x-direction. The red dashed line shows the non-bonded nearest neighbor pairs along x and y-direction and corresponding Boltzmann weights are represented by τ_x and τ_y; (c) Model C is same as model B, but the solvent interaction gradient inside an entropic trap (region II) acts along the transverse direction (y-axis); (d) Model D is same as the model C, but the solvent interaction gradient has the reverese sign in compare to model C.

homogeneity inside the channel, we introduce three different regions (I, II, and III) of different dimensions and solvent quality (good or poor) in presence (or absence) of entropic trap as shown in Fig. 2.1(a-d). For the sake of simplicity, we introduce four different models, namely, Model A, B, C, and D depending on the solvent gradient (along the channel or perpendicular to the channel) and entropic trap Fig. 2.1 (a-d). Here, we study migration properties in absence (Fig. 2.1(a): model A) and in presence (Fig. 2.1(b): model B) of entropic trap having the solvent interaction gradient along x-axis while the other parameters remain constant.

In model A and B (Fig. 2.1 (a,b)), region I and III have the dimension of length (l_1) and width (h) 14 and 12 lattice units, respectively. Whereas, the middle region II of the model A has dimension of length (l_2) and width (h) 10 and 12 lattice units, respectively. The Model B has an entropic trap of dimension of length (l_2) 10 and depth (d) 10 lattice units. The interest here is to study the migration of a polymer chain from region I to region III and delineate the role of an entropic trap on the free energy barriers and the migration time. Here, we introduce a solvent interaction gradient ($\Delta\epsilon = \frac{\epsilon}{l_2}$) along the channel direction (x-axis). The strength of the interaction associated with nearest neighbor pairs in this region may be defined as $\epsilon(l_2^i) = l_2^i \Delta\epsilon(l_2)$, where $i = 1, 2, 3.....10$. It may be noted here that the first layer of region II has the value of $\epsilon(l_2^1 = 1) = 0$ (good), whereas the last layer of region II has the value of $\epsilon(l_2^{10} = 10) = -1$ (poor) for $\Delta\epsilon = -0.1$. Region II is the interface (indicated by thin and thick lines in Fig. 1) between the two regions I and III as the solvent of region III follows the solvent quality of last layer of region II depending on the value of $\Delta\epsilon$. It is pertinent to mention here that for $\Delta\epsilon = 0.0$ the solvent quality remains good across all regions of the channel in both models A and B. Here, we show that this simple form of solvent gradient captures the essential physics of migration by considering different nearest neighbor interactions arising in the x- and y-directions.

In region I and III the Boltzmann weight for the non-bonded nearest neighbor interaction is $\tau = \exp(-\beta\epsilon)$. In the region II, the non-bonded nearest neighbor interaction is uniform along y-direction and has weight

$$\tau_y(x) = \exp(-\beta\epsilon(x)). \tag{2.2}$$

However, the non-bonded nearest neighbor involved in between x and $(x \pm 1)$ layers, the Boltzmann weight can be expressed as,

$$\tau_x(x) = exp(-\frac{\beta}{2}(\epsilon(x) + \epsilon(x \pm 1))) \tag{2.3}$$

The model B is similar to the model A, except it has an entropic trap

($l_2 = 10$ lattice units and $d = 10$ lattice units) in the region II as shown in Fig. 2.1(b)).

In this work, the canonical partition function of the model systems can be expressed as:

$$Z^x = \sum_{(N_{p1},N_{p3},N^x_{p2},N^y_{p2},x)} C(N_{p1}, N_{p3}, N^x_{p2}, N^y_{p2}, x) \tau_x^{N^x_{p2}} \tau_y^{N^y_{p2}} \tau^{N_{p1}} \tau^{N_{p3}}. \quad (2.4)$$

Where N_{p1} and N_{p3} are the number of non-bonded pairs formed in the regions I and III respectively. N^x_{p2} and N^y_{p2} are the the non-bonded nearest neighbor contacts along x and y- direction, respectively in the region II.

The solvent quality inside the channel is good and poor in the Model C and D (Fig. 2.1 (c,d)), respectively. However, the solvent gradient interaction is perpendicular to the direction of migration. In the model C, the solvent gradient interaction decreases with the depth of the entopic trap, whereas in the model D, it increases with the depth of the entropic trap. This is analogous to the situation where the quality of the solvent is relatively poor (low temperature regime) at the bottom layer of the model C. Contrary to the model C, the entropic trap of the model D has relatively good solvent ($\epsilon = 0$) at the bottom *i.e* the bottom layer is at high temperature. In both the models C and model D, the gradient ($\Delta\epsilon = \frac{\epsilon}{d}$) is defined in such a way that the non-bonded pair at the bottom layer contributes $-1 < \epsilon < 0$. For these cases, interactions at any layer inside the entropic trap may be defined as $\epsilon(d^i) = \epsilon + d^i\Delta\epsilon$, where $i = 1, 2, 3.....10$. The value of $\Delta\epsilon$ lies between 0 to -0.1 for the model C and 0 to 0.1 for model D.

The non-bonded nearest neighbor interaction inside the entropic trap remains constant along the x-direction and its Boltzmann weight is given by,

$$\tau_x(y) = exp(-\beta\epsilon(y)). \quad (2.5)$$

Whereas if any pair is taking place between y-th and $(y \pm 1)$-th layers,

then we express the Boltzmann weight as,

$$\tau_y(y) = exp(-\frac{\beta}{2}(\epsilon(y) + \epsilon(y \pm 1))) \tag{2.6}$$

In the equilibrium framework of statistical mechanics, it is difficult to study the migration of polymer chain. However, if the process is slow in such a way that the system achieves the quasi-static equilibrium at a given instant of time. In such situation, it is possible to study the dynamics of the system by using the Fokker-Planck equation. The basic ingredient of the Fokker-Planck equation is the free energy of the system at any instant of time for a given value of x. For this, we assume that the polymer is migrating from the region I to region III and the free energy of the system may be obtained by progressively fixing one end of the polymer from $x = 0$ to $x = 38$, whereas other end of the polymer is free to be anywhere inside the channel. We used the exact enumeration technique [82] to calculate the partition function for a given value x by using the following equation:

$$Z^x = \sum_{(N_{p1}, N^x_{p2}, N^y_{p2}, x)} C(N_{p1}, N^x_p, N^y_p, x) \tau_x^{N^x_{p2}} \tau_y^{N^y_{p2}} \tau^{N_{p1}} \tag{2.7}$$

where N^x_{p2} and N^y_{p2}, are the number of nearest neighbor contacts along x-direction and along y-direction, respectively inside the entropic trap. $C(N_{p1}, N^x_{p2}, N^y_{p2}, x)$ is the number of distinct configurations having N_{p1} contacts in the channel and $N_{p2}(= N^x_p + N^y_p)$ contacts in the entropic trap. The free energy of the system for a given value of x is given by

$$F^x = -Tlog(Z^x). \tag{2.8}$$

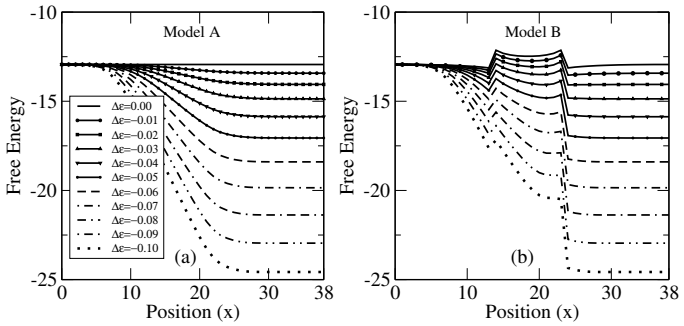

Figure 2.2. Variation of the free energy with anchoring coordinate (x) for different solvent interaction gradient ($\Delta\epsilon$): (a) for model A (b) for model B.

2.3 Free energy landscape

The migration process may be understood if one has the complete information of the free energy associated with each region of the channel. In order to have a better understanding the effect of the entropic confinement on the migration process, we systematically calculate the free energy of the system as a function of x, where one end of the chain is anchored. It may be noted that in both models A and B, region I has a good solvent ($\epsilon = 0$) and gradient acts along the x-direction and they differ only in terms of entropic trap. For model A, when $\Delta\epsilon = 0.0$, the free energy remains constant throughout the channel Fig. 2.2(a). This implies that monomer-monomer attractions remain absent ($\epsilon = 0$) throughout the channel for region I, II, and III. Now we systematically vary the nearest neighbor attraction among the monomers at the interval of 0.1 in the region III. This gives rise to the solvent interaction gradient in the region II. As $\Delta\epsilon$ decreases, one end of the region II (near to the poor side) becomes poorer compare to the side which is close to the good solvent. As a result, the polymer prefers to move towards region II as free energy decreases and approaches the free energy of region III. The migration seen in model A closely resembles the characteristics of voltage driven translocation [86]. The presence of entropic trap (model B) shows some interesting behavior which can be seen in Fig. 2.2(b). The appearance of

free energy barrier for low $\Delta\epsilon$ and change in slope in free energy curve at the interfaces of region I & II and region II & III are some notable observations which may influence the migration behavior inside the channel. For $\Delta\epsilon = 0.0$, where the solvent quality throughout the channel remains good in nature, the appearance of free energy barrier at the interfaces of region I & II and region II & III is solely due to the entropic trap. As $\Delta\epsilon$ decreases, the solvent quality of the region II becomes more poorer compare to region I. The decrease in $\Delta\epsilon$ favors the migration process easier. The free energy decreases gradually from region I to region II and approaches the free energy of region III.

For both models the gradient enhances the migration process, however, the entropic trap reduces the process in comparison to model A. To substantiate it, one can calculate the average time involved in migration between the initial (region I) and final stage (region III). Since the free energy of the polymeric system is known, one can employ Fokker-Planck formalism to obtain the migration time from region I to region III. The governing equation is given by

$$\frac{\partial}{\partial t}p(x,t) = L(x)p(x,t), \tag{2.9}$$

where $p(x,t)$ is the probability distribution. $L(x)$ is the Fokker-Planck operator described by

$$L(x) = \frac{1}{b^2}\frac{\partial}{\partial x}D(x)exp(-F(x))\frac{\partial}{\partial x}\exp(F(x)), \tag{2.10}$$

where $F(x)$ is the free energy of the polymer. $D(x)$ is the diffusion coefficient and b is the bond length. Following the method developed in Ref. [77], we set $D(x) = 1$. Since, the present study is confined on the lattice, we assigned the bond length to be unity and the migration time has been

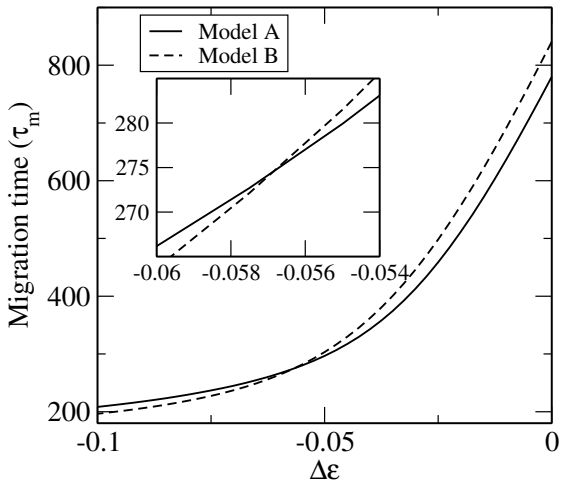

Figure 2.3. Variation of the migration time (τ_m) with $\Delta\epsilon$ for model A and model B. In the inset we show the region where migration time for the model B exceeds the model A.

expressed in the following discrete form:

$$\tau_{(x=0;x=38)} = \sum_{x'=0,1,2,...38}^{38} \Delta x^{'} \exp(F(x^{'})) \sum_{x''=0}^{x^{'}} \Delta x^{''} \exp(-F(x^{''})) \quad (2.11)$$

Here, the first summation adds the contribution of free energies from $x^{'} = 0, 1, 2.., 38$ to $x^{'} = 38$, whereas the second summation sums up the free energy contributions from $x^{''} = 0$ to $x^{'}$. Here, we have taken $\Delta x^{"} = \Delta x^{'} = 1$ in lattice units.

The migration time required to reach region III from region I for model A and B are shown in Fig. 2.3 as a function of $\Delta\epsilon$. It is evident from the plots that for $\Delta\epsilon = 0$, the free energy barrier arising due to the entropic trap (model B) offers slow migration in comparison to the model A. The decrease in $\Delta\epsilon$ corresponds to the reduction in the free energy which in turn expedites the migration towards the region III. One of the interesting

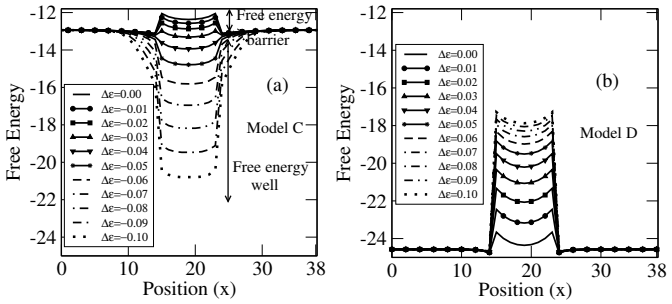

Figure 2.4. The free energy landscape for different values of $\Delta\epsilon$: (a) for the model C; (b) for the model D. The arrows shown in Fig. (a) indicate the free energy barrier and free energy well.

observations can be noted that for both models the migration time (τ_m) decreases, however, around $\Delta\epsilon \sim -0.057$, the migration time for model A exceeds in comparison to the model B. This may be explained on the basis of subtle competition between increase in entropy and solvent interaction gradient. We may substantiate this result with the argument that due to entropic trap polymer exposure in the gradient (region II) also increases, which eventually drives the polymer towards region III. As a result one observes less migration time for model B compared to model A for $\Delta\epsilon < -0.057$. As the anchor sites move away from the entropic trap, the migration time approaches monotonically towards model A.

It would be interesting to study the effect of transverse gradient which may be present in the entropic trap. In this context two situations may arise: (i) the channel has a good solvent ($\epsilon = 0$), while the entropic trap contains a relatively poor solvent (model C); (ii) the channel contains poor solvent ($\epsilon = -1$), whereas the entropic trap has a relatively good solvent (model D). In both cases we assigned transverse nearest neighbor interaction gradient by substituting $-0.1 < \Delta\epsilon < 0$ for model C and $0.1 < \Delta\epsilon < 0$ for model D. As a result the nearest neighbor attraction at the bottom layer of the entropic trap will have the value $-1 < \epsilon < 0$ for model C and $0 > \epsilon > -1$ for the model D. This ensures decrease in solvent gradient with depth of the trap for the model C and increases in

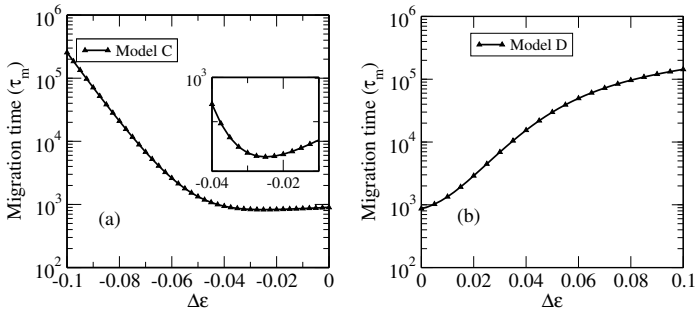

Figure 2.5. (a) Variation of the migration time with $\Delta\epsilon$. (a) for the model C; (b) for the model D. The inset of Fig. (a) shows the minimum of migration time for model C; (b) Same as (a), but for the model D.

solvent gradient with the depth of the entropic trap for the model D. This is analogous to the situation where the bottom layer of entropic trap is at lower temperature compared to the temperature of the channel. Contrary to model C, the channel of model D has lower temperature compare to the entropic trap.

Fig. 2.4 (a) shows the free energy landscape (for model C) as a function of x where one end of the polymer is anchored. For $\Delta\epsilon = 0.0$, the solvent quality remains uniform in the entropic trap as well as across the channel. One can observe the barrier in the free energy landscape which is arising due to the confinement imposed by the entropic trap. Because of the entropic trap, there is a significant decrease in the configurational entropy of the polymer chain which gives rise to the barrier. As $\Delta\epsilon$ decreases, the solvent quality of the trap turns out to be poorer compare to the solvent quality of the channel. As a result, there is a decrease in the free energy arising due to the solvent gradient which overcomes the entropic barrier. A further decrease in $\Delta\epsilon$ transforms the free energy barrier to the well. It would be interesting to note that both free energy barrier and well hinders the polymer movement across the channel. The time involved in the migration process from region I to region III is minimum around $\Delta\epsilon \sim -0.03$. This corresponds to a net balance between entropic barrier and solvent interaction gradient to the free energy.

Since the channel in model D contains poor solvent all across the channel for $\Delta\epsilon = 0$, one can see the similar free energy barrier as seen in model C. However, as solvent quality in the entropic trap becomes good ($\Delta\epsilon > 0$) the barrier height increases across the trap (Fig. 2.4). Unlike model C, here the barrier height always increases. As a result one expects larger migration time. The migration time for model C and D is shown in Fig. 2.5. The model C shows the non-monotonic dependence on $\Delta\epsilon$ (Fig. 2.5(a)). When $\Delta\epsilon$ decreases ($\Delta\epsilon < 0$), free energy well is formed across the trap. Here, polymer acquires the configuration of the globule state and remains confined in the trap. As a result the time required for the migration is found to be large. As $\Delta\epsilon$ increases, the solvent quality of the trap tends towards the good solvent and thus globule gets destabilized due to increase in configurational entropy. In contrast to the model C, the model D shows the migration time monotonically increasing with $\Delta\epsilon$ Fig. 2.5 (b). This may be understood by making the solvent quality good inside the trap and leads to the conformation of the polymer chain in the swollen state. As the $\Delta\epsilon$ increases the trap becomes more repulsive and the free energy barrier increases. An increase in barrier height further enhances the migration time.

It is interesting to note that the migration time is nearly equal to $\Delta\epsilon = 0$ for both models C and D. This indicates that for the good solvent channel (model C with $\Delta\epsilon = 0$) and poor solvent channel (model D with $\Delta\epsilon = 0$), the polymer takes almost the same time. This is because the appearance in free energy barrier at $\Delta\epsilon = 0$ is solely entropic and hence the same for both models. The presence of gradient ($\Delta\epsilon > 0$) inside the entropic trap makes the migration process slow.

2.4 Configurational properties of polymer during migration

It would be interesting to investigate how the configurational properties of the polymer change due to the solvent interaction gradient in the en-

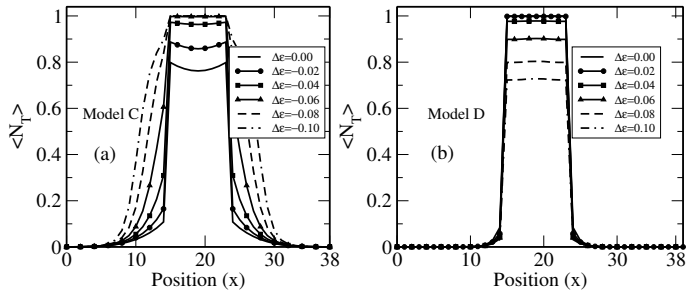

Figure 2.6. The average number of monomers inside the trap ($\langle N_T \rangle$) for different $\Delta\epsilon$: (a) for model C; (b) for model D.

tropic trap. For this, we first calculate the average number of monomers ($\langle N_T \rangle$) inside the trap as a function of x. It may be pointed here that the trap coordinates are lying within $15 < x < 24$. The figure Fig. 2.6 (a) shows the fraction of monomers inside the trap (model C) as a function of x which is almost negligible when the anchored sites are far away from the trap. As the anchor site approaches towards the trap, $\langle N_T \rangle$ starts increasing. As $\Delta\epsilon$ decreases, a part of the polymer favors to be inside the trap and tends to acquire the globule state. This behavior is also evident from the free energy curve Fig. 2.4 (a). where the free energy decreases before the anchor site reaches near the trap. This corresponds although a fraction of segments remains in the swollen state due to the anchor site, however, the remaining segment inside the trap forms the globule. Fig. 2.6(b) shows the variation of $\langle N_T \rangle$ with x for model D. Here, we focus when the polymer is mostly confined in the region II *i.e.* inside the trap. Here, the polymer remains in the globule state around the anchor sites (outside the trap) and does not experience any effect of solvent in the trap. When the anchor site is forced to be inside the trap, a part of the polymer segment remains in the swollen state (inside the trap) whereas the remaining part will be outside the trap, but in the globule state. When $\Delta\epsilon \to 0$ (*i.e* solvent in the channel and inside the trap remain the same), it acquires the globule state inside the trap.

The variation in shape of polymer in terms of the radius of gyration

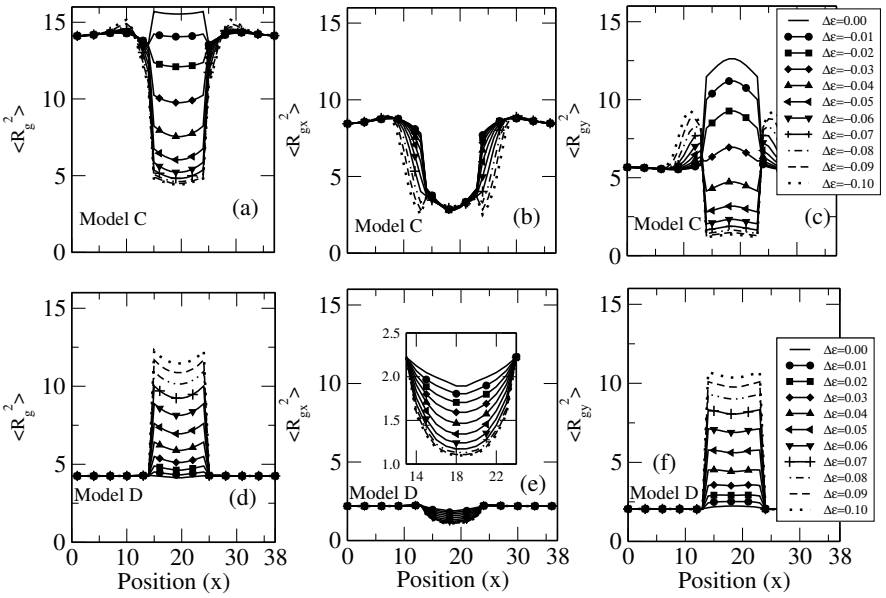

Figure 2.7. (a) Variation of radius of gyration ($\langle R_g^2 \rangle$) with x for different $\Delta\epsilon$ for model C; (b) Variation of x-component of radius of gyration ($\langle R_{gx}^2 \rangle$) with x for different $\Delta\epsilon$ for model C; (c) Variation of y-component of radius of gyration ($\langle R_{gy}^2 \rangle$) with x for different $\Delta\epsilon$ for model C; (d-f) Same as Fig. (a,b,c), but for model D.

($\langle R_g^2 \rangle$) as a function of anchoring coordinates (x) for model C and D are shown in Fig. 2.7 (a) & (d), respectively. For both models, we observe slight increase in $\langle R_g^2 \rangle$ near the edge of the trap compare to the middle of the trap. This is because, near the edge the polymer has the option to spread along y-direction and that maximizes the monomer density at the edge. As one moves towards the center of the trap, polymer can spread in all directions and thus $\langle R_g^2 \rangle$ decreases for model C and increases for model D Fig. 2.7 (a) & (d). At $\Delta\epsilon \approx -0.03$ which corresponds to the minimum migration time, also shows the least variation in $\langle R_g^2 \rangle$ all across the channel for model C. As $\Delta\epsilon$ decreases the quality of the solvent becomes poorer for model C and hence $\langle R_g^2 \rangle$ decreases. As a result the migration time also increases. On the other hand, in model D the solvent quality tends towards a good solvent with $\Delta\epsilon$, and thus $\langle R_g^2 \rangle$ tends to its swollen state value.

Since the microscopic variation in shape arising due to confinement is not quite apparent from Fig. 2.7 (a) & (d), therefore, we study the variation of polymer shape in terms of the x and y components of radius of gyration as a function of x. The variation in $\langle R_{gx}^2 \rangle$ and $\langle R_{gy}^2 \rangle$ are shown in Fig. 2.7(b-c) & Fig. 2.7(e-f) for model C and D respectively. One can notice from the plots that the entropic trap in presence of the solvent interaction gradient affects $\langle R_{gy}^2 \rangle$, whereas $\langle R_{gx}^2 \rangle$ remains almost the same. It may be noted that the model C has relatively poor solvent inside the trap, and thus there is a natural tendency to minimize its free energy, even if the anchor site is outside the trap. This may be seen in the variation of both $\langle R_{gx}^2 \rangle$ and $\langle R_{gy}^2 \rangle$, when the anchor sites are outside the trap. The most interesting observation is the increase in $\langle R_{gy}^2 \rangle$ as a function of x and then sudden decrease for $\Delta\epsilon < -0.03$. This may be understood as the bottom surface of the trap has a poor solvent (less temperature) and thus a major fraction of the polymer chain prefers to stay in the globule state, whereas its anchor site is outside the trap. As a result, the polymer is forced to acquire the conformation along the side of the trap (y-axis) and thus $\langle R_{gy}^2 \rangle$ increases. In contrast to model C, model D shows Fig. 2.7 (c,f) gradual decrease in $\langle R_{gx}^2 \rangle$ and increase in $\langle R_{gy}^2 \rangle$ as a function of x inside the trap for a given chain length. When $\Delta\epsilon = 0$, the solvent all across the channel is poor and the polymer remains in the globule state inside the trap, as well as outside the trap. This is evident from Fig. 2.7 (c) and Fig. 2.7 (f) where both components of $\langle R_g^2 \rangle$ remains almost the same. As $\Delta\epsilon$ increases, the solvent inside the trap becomes good, the y-component of $\langle R_g^2 \rangle$ increases. In this situation, polymer acquires the "mushroom" shape in such a way that the major fraction of the polymer prefers to be outside the trap in the globule form [87]. This in turns reduces the $\langle R_{gx}^2 \rangle$ which approaches towards 1 as shown in inset of Fig. 2.7 (e).

2.5 Summary

In this chapter, we have studied the effects of solvent interaction gradient inside the entropic trap on the migration of polymer. Employing the exact enumeration technique and by varying the anchoring sites of one end of the anchored polymer, we have studied the migration of polymer from one side (region I) to the other (region III) by assuming that the system remains in the quasi-static equilibrium condition. We have considered solvent interaction gradient both in parallel and perpendicular to the migration direction in region II. The free energy landscape of model A (without entropic trap) and model B (with entropic trap) differs significantly and shows the influence of entropic trap. Using the Fokker-Planck equation, we obtain the migration time which shows that as $\Delta\epsilon$ decreases, the migration time decreases. The exact calculation based on the short chain revealed that for a certain value of $\Delta\epsilon$, the entropic trap may reduce the migration time.

In contrast to model A and B where the gradient is taken along the x-axis, we have explored the effect of transverse gradient (y-axis) in presence of entropic trap in model C and D. We have considered two possibilities: the channel has a good solvent (high temperature) and solvent confined in an entropic trap is poor (low temperature) and *vice versa*. We have imposed a linear solvent interaction gradient and studied the migration behavior of polymer chain from region I to region III in presence of an entropic trap. In this case, the migration time shows a non-monotonic behavior as a function of solvent interaction gradient for model C, whereas monotonic increase in case of model D. At $\Delta\epsilon \approx -0.023$, the free energy barrier / well vanishes and at this value the migration time is found to be the minimum. Interestingly, model D has the free energy barrier which increases with $\Delta\epsilon$ and hence migration time increases monotonically. We have also explored the variation in shape of polymer inside the trap for model C and D. We observed that the entropic trap has significant impact on the y-component of $\langle R_g^2 \rangle$, whereas x-component remains almost the

same.